Cancer Immunology, Immunotherapy (2025) 74:201
https://doi.org/10.1007/s00262-025-04045-9

RESEARCH

Recombinant antibodies from clonally expanded cancer-associated plasma cells

Wonkyung Kim[1,2] · Ji-Hye Oh[3] · Chae Won Park[1,2] · Hyori Kim[4] · Young Gwang Kang[1,2] · Da Eun Oh[3] · Hee Jin Lee[2,5] · Ji Hun Kim[6] · Chang Ohk Sung[1,2,3]

Received: 29 October 2024 / Accepted: 7 April 2025

Abstract

Although the clinical significance of plasma cells within tumors has been recognized, studies on the development of plasma cells and the characteristics of the antibodies they secrete within the tumor microenvironment remain limited. We investigated the properties of plasma cells within cancer tissues using single-cell RNA and single cell B cell receptor sequencing. We characterized plasma cells exhibiting clonal expansion and synthesized the antibodies produced by these cells, confirming the clinical relevance of immunoglobulin H (IGH) isotypes. Plasma cells comprised approximately 5% of the total immune cell population within the tumor; clonal expansion was more prevalent in plasma cells than in B cells. Among plasma cells, the most frequent immunoglobulin isotype was IGHG1 and IGKC. We synthesized six recombinant antibodies, including those from the largest clonal plasma cells. Two antibodies that formed clones showed membranous staining in cancer cells. The cancer cells that metastasized to the lymph node showed a loss of expression as observed by immunohistochemistry. Analysis of bulk RNA sequencing data from 1078 patients with breast cancer revealed that tumor-infiltrating plasma cells expressing IGHG1 were associated with favorable prognoses. These tumors exhibited increased B cell receptor diversity, immunogenic mutation, and intratumoral heterogeneity. This study suggests the potential for discovering cancer-associated antibodies derived from intratumoral plasma cells.

Keywords Recombinant antibody · Plasma cell · Cancer · Single-cell sequencing · B cell receptor

Abbreviations

Ab	Antibody
BCR	B cell receptor
scRNA-seq	Single cell RNA sequencing
scBCR-seq	Single cell BCR sequencing
TIL	Tumor infiltrating lymphocytes

Introduction

The discovery of cancer-associated antibodies is crucial in diagnosing and treating cancer because these antibodies can identify and/or target antigens that are exclusively present on or overexpressed in cancer cells [1]. There are various methods of identifying cancer-specific antibodies; however, these

✉ Hee Jin Lee
backlila1@amc.seoul.kr

✉ Ji Hun Kim
jihkim@kaist.ac.kr

✉ Chang Ohk Sung
co.sung@amc.seoul.kr

1 Department of Medical Science, Brain Korea 21 Project, Asan Medical Institute of Convergence Science and Technology, University of Ulsan College of Medicine, Seoul, Republic of Korea

2 Department of Pathology, Asan Medical Center, University of Ulsan College of Medicine, 88, Olympic-ro 43-gil, Songpa-gu, Seoul 05505, Republic of Korea

3 Bioinformatics Core Laboratory, Convergence Medicine Research Center, Asan Medical Center, Asan Institute for Life Sciences, Seoul, Republic of Korea

4 Antibody Development Core Laboratory, Convergence Medicine Research Center, Asan Medical Center, Asan Institute for Life Sciences, Seoul, Republic of Korea

5 NeogenTC Corp., Seoul, Republic of Korea

6 Graduate School of Medical Science and Engineering, Korea Advanced Institute of Science and Technology, Daejeon 34141, Korea

Published online: 13 May 2025

methods often involve significant technical challenges and can be labor-intensive. B cells recognize antigens through B cell receptors (BCRs), and the diversity of BCRs is generated by V (variable), D (diversity), or J (joining) gene (V(D)J) recombination, somatic hypermutation, and class switch recombination during B cell development and differentiation [2]. Therefore, theoretically, the maximum number of antibodies produced by human plasma cells is upward of 10^{13}.

Tumor-infiltrating lymphocytes (TILs) have recently been characterized in several human cancers using single-cell RNA sequencing (scRNA-seq) [3–6]. However, information on tumor-infiltrating plasma cells is still lacking. Intratumoral plasma cells have also recently been identified as a key determinant of survival in patients undergoing immunotherapy treatment for cancer [7]. Additionally, the infiltration of intratumoral plasma cells has been reported to be associated with favorable prognoses in various cancers, including breast cancer [8–11]. This finding suggests that antibodies produced by plasma cells play a role in anti-tumor activity, given that the primary function of plasma cells is antibody production.

To investigate the characteristics of plasma cells within tumor tissue and the antibodies they produce, we performed scRNA-seq and scBCR-seq on breast cancer tissues. This approach allowed us to determine the BCR repertoire and transcriptional characteristics of plasma cells, laying the potential foundation for further clinical applications of cancer-associated antibodies in immunotherapy.

Materials and methods

Patients and tissue specimens

After obtaining written informed consent, breast cancer tissue samples were surgically harvested from three female patients treated without neoadjuvant systemic chemotherapy at the Asan Medical Center, Seoul, Korea, in 2021. This study was performed in accordance with the Declaration of Helsinki and was approved by the institutional review board (IRB) of Asan Medical Center (IRB no. 2015–0438). For subtyping, cancer tissues were immunohistochemically stained with antibodies against estrogen receptor (ER; diluted 1:200; NCL-L-ER-6F11, Novocastra, Newcastle-upon-Tyne, UK), progesterone receptor (PR; diluted 1:200; NCL-L-PGR-312, Novocastra, Newcastle-upon-Tyne, UK), and human epidermal growth factor receptor 2 (HER2; diluted 1:8; 88–4422, Ventana Medical Systems, Tucson, AZ, USA). ER and PR were evaluated using the Allred score system, in which their levels were regarded as positive if ≥ 1% of tumor nuclei were stained. Hormone receptor-positive tumors were defined as those with positive ER and/or PR staining. Silver in situ hybridization for the *HER2* gene was performed in cases with HER2 immunohistochemical staining results OF ≥ 2. The slides were evaluated for the levels of stromal TILs using full sections in 10% increments (if < 10%, 0, 1, or 5% level criteria were used) [12].

scRNA-seq and scBCR-seq sequencing

Sample multiplexing single cell sequencing libraries were prepared for 10 × Genomics single-cell 5′ gene expression and V(D)J sequencing according to the protocol provided by the 10 × Genomics chromium single-cell immune profiling platform. The cell loading numbers for the three samples, BC20128, BC20131, and BC20136, were 9,280, 10,080, and 10,472, respectively, and sequencing data for a total of 5,735 cells were generated from the multiplexed library, which was sequenced using an Illumina NovaSeq 6000. Demultiplexing by genotyping, gene expression count data, and BCR repertories with reconstruction of full-length BCR sequences were performed using Cell Ranger v6.1.1 from the multiplexed scRNA-seq and scBCR-seq.

Processing of scRNA-seq

The 10 × Genomics scRNA-seq data was processed using CellRanger (version 6.1.1) with the GRCh38 genome. Based on a filtered gene-cell count matrix obtained using CellRanger's default cell calling algorithm, we performed the standard Seurat clustering (version 5.0.1 in R 4.3.2) workflow as described below; raw expression values were normalized and log transformed (normalization method = "LogNormalize"). Low-quality cells were excluded by filtering out those with < 200 or > 6,000 detected genes. We also filtered out cells with mitochondrial counts > 20% [13, 14]. Ambient RNA-contaminated cells were excluded using demuxlet. Normalization was performed using the "NormalizeData" function in Seurat with the method set to "LogNormalize." Highly variable features were identified using the "FindVariableFeatures" function with the "vst" method; "nfeatures" = 2000. Batch effects were corrected using the Harmony algorithm through "RunHarmon." Dimensionality reduction was performed using principal component analysis using the "FindNeighbors" function with the Louvain algorithm applied with a resolution of 0.6 to iteratively group cells using the "FindClusters" function. We generated uniform manifold approximation and projection (UMAP) with clusters using the "Run UMAP" function. Thereafter, the following confounding factors were regressed using the "ScaleData" function: cell cycle scores output using the "CellCycleScoring" function, percentage of mitochondrial DNA, patient identification, and the number of unique molecular identifiers. Clustering was performed at a resolution of 0.6, and cell types were annotated based on known marker genes from the CellMarker 2.0 database specific to breast cancer.

Processing of scBCR-seq

Raw scBCR-seq data were aligned using CellRanger (version 6.6.1) with GRCh38 V(D)J references provided by 10 × Genomics. Aligned single-cell BCR data were reannotated using Dandelion (version 0.3.5). The Seurat object was converted to a Scanpy object for integration with BCR data. This integration facilitated a comprehensive analysis using both gene expression and receptor information. Clonal analysis was performed using the ddl.tl.find_clones function, which identifies clones based on identical V- and J-gene usage, complementarity determining region 3 sequence length, and sequence similarity, using V(D)J chain junctional/complementarity determining region 3 sequences with at least 85% sequence similarity based on a number of amino acid mismatches. Clones were further analyzed to construct networks using the "ddl.tl.generate_network" function, which uses amino acid sequences to build Levenshtein distance matrices. Using these distance matrices, the BCR network was constructed by generating a minimum-spanning tree on the adjacency matrix for each clone/clonotype, creating a simple graph with edges representing the shortest edit distance between a B cell and its nearest neighbor.

Cell–cell communication

We used CellChat (version 2.1.0) to infer ligand-receptor-based interactions between cells. CellChat inferred ligand-receptor interactions on integrated scRNA-seq data according to the standard procedures [15]. The expression matrix and cell type information were imported into CellChat, and we computed the intercellular communication probability between each module and other cell populations using the CellChat "computeCommunProb," "computeCommunProbPathway," and "aggregateNet" functions. To determine the senders and receivers in the network, the "netAnalysis_signalingRole" function was applied to the netP data slot. The ligand-receptor pairs based on cell type were identified using the "netVisual_bubble" function. The communication probability between two cell types was calculated using the computeCommunProb function in CellChat. This probability is a quantitative measure of the interaction strength between ligands and receptors and is calculated based on the average expression values of specific ligands in one cell type, their corresponding receptors in another cell type, and any associated cofactors.

Pseudotime trajectory analysis

Cell differentiation was inferred for B and plasma cells using Monocle2 (version 2.30.0) with default parameters. Integrated gene expression matrices for each cell type were exported from the Seurat object into Monocle to construct a CellDataSet. All variable genes defined by the "differentialGeneTest" function (q-val cutoff < 0.05) were used for cell ordering with the "setOrderingFilter" function. Dimensionality reduction was performed using the DDRTree reduction method with no normalization in the reduceDimension step.

Recombinant antibody production from plasma cells based on scBCR-seq

The variable regions for both heavy and light chains identified by scRNA-BCR sequencing were synthesized (IDT Inc., USA) and cloned into pCEP4 (Invitrogen, USA) expression vectors containing a leader sequence of human immunoglobulin kappa chain and rabbit IgG constant regions. These expression vectors were then transfected into Expi293F (Gibco, USA) cells for protein production. Additionally, 40 mL of 25 kDa linear polyethylenimine (PEI, Polysciences, USA) was used as the transfection reagent. Following transient expression, the cells were grown in Expi293F Expression Medium (Gibco, USA) for five days. The rabbit IgG proteins were purified from the culture supernatant using affinity chromatography with MabSelect SuRe resin (Cytiva, USA). Protein samples were prepared by adding or omitting 10 × reducing agent (Invitrogen, NP0004) to a mixture of 1 μg of protein and 4 × sample buffer (Invitrogen, NP0007). Protein integrity and purity were assessed using sodium dodecyl-sulfate polyacrylamide gel electrophoresis followed by Coomassie Brilliant Blue staining, and protein concentration was determined using a bicinchoninic acid assay.

Immunohistochemistry using recombinant synthetic antibodies

Formalin-fixed paraffin-embedded tumor tissues corresponding to scRNA sequencing were used for immunohistochemistry studies of the synthesized antibodies. The specific formalin-fixed paraffin-embedded tissue sections were immunohistochemically stained for the synthesized antibodies (1:200) using an OptiView 3, 3′-diaminobenzidine Immunohistochemistry Detection Kit on a BenchMark XT automatic immunostaining device (Ventana Medical Systems, Tucson, AZ, USA) according to the manufacturer's instructions. As negative controls, tonsil tissue and a tissue microarray comprising 103 normal breast tissues were used.

Plasma cell scoring and the cancer genome atlas (TCGA) bulk RNA-seq with clinical information

The plasma cell scores were calculated using the scRNA-seq data by identifying differentially expressed genes between plasma cells and other cell types and then applying the plasma cell signature gene set to the bulk RNA-seq data.

Deconvolution using the plasma cell signature gene set was performed with the singscore R package v1.20.0. For TCGA bulk RNA-seq data, normalized gene expression data (illuminahiseq_rnaseqv2-RSEM_gene_normalized) and corresponding clinical data for 8,469 cancer tissues including 1,079 breast cancers were downloaded from illuminahiseq_rnaseqv2-RSEM_gene_normalized. The cancer types and the number of samples for each cancer type are described in our previous study [13, 14]. Immunogenic mutation number, intratumoral heterogeneity score, aneuploidy score, BCR diversity scores, and plasma cell CIBERSORT score were obtained from https://gdc.cancer.gov/about-data/publications/panimmune [16]. Immunogenic mutations refer to mutant proteins (neoantigens) among single nucleotide, insertion, or deletion mutations predicted to bind to major histocompatibility complex (MHC) proteins and elicit an immune response.

Measurement of IGH isotype abundance

Raw RNA-seq data (FASTQ files) were downloaded from the Cancer Genomics Hub (https://cghub.ucsc.edu/) [17] for breast cancer ($n = 1,079$), approved by the National Institutes of Health (no. 30444–1). The modified hg38 human reference genome was used as the reference genome, masked at the IGK@ locus on chromosome 2 (chr2 88,833,331–90,359,502), IGL@ locus on chromosome 22 (chr22 22,010,000–23000000), and IGH@ locus on chromosome 14 (chr14 104,930,000–106630000). Raw RNA-seq data were then aligned with the masked reference genome using TopHat2 (2.0.12 version, default option) [18] with Bowtie2 (2.0.6 version) [19]. Next, the unmapped reads of the Binary Alignment Map file, irrespective of the status of the other read of the pair, were collected and used for further analysis. SAMtools (0.1.19 version) and Picard tools (1.119 version) were used to convert the unmapped Binary Alignment Map files to unmapped FASTQ format files [20]. Then, the unmapped FASTQ files were mapped to the reference FASTA files of IGH isotypes, including G1, G2, G3, G4, A1, A2, D, E, M, GP, and EP1, to obtain read counts, which were adjusted by the length of each IGH isotype to calculate the normalized read count.

Microscopy imaging data

Hematoxylin and eosin-stained histology images of 744 breast cancer tissues were obtained from Berkeley Cancer Morphometric Data (http://tcga.lbl.gov/biosig/tcgadownload.do). The intratumoral plasma cell infiltration level was classified by a pathologist (C.O.S) into four categories, including no/little, mild, moderate, and marked infiltration, based on the hematoxylin and eosin-stained histologic images.

Statistical analysis

The Wilcoxon-rank sum test or Student's t-test was used to compare the intergroup differences in continuous variables. Spearman's correlation test was used to measure the correlation between pairs of variables. Linear regression analysis was used to examine the relationship between a single dependent and one or more independent variables. Survival analysis was performed using the log-rank test and univariate and multiple Cox proportional hazards regression analyses. All statistical analyses were performed with R v4.1.3.

Results

Study design and single-cell transcriptional profiling

Based on the idea that plasma cells within the tumor microenvironment can produce cancer-associated antibodies during the anti-tumor immune response (Fig. 1A), we conducted a study to elucidate the characteristics of these plasma cells and the antibodies they generate. We performed scRNA-seq and scBCR-seq on breast cancer tissue specimens from three patients, two with hormone receptor-positive cancer and one with triple-negative breast cancer (Fig. 1B). Of the 5,735 sequenced cells, 4,846 cells that passed quality control during data preprocessing were included in the final analysis. When annotating cell types from the scRNA-seq, various immune and cancer cells were identified (Fig. 1C and Supplementary Table 1). B and plasma cells each expressed their respective known markers well (Fig. 1D), and plasma cells accounted for 1–5% of the total cells in the tissue specimens (Fig. 1E). For scBCR-seq sequencing, immunoglobulin chain pairing analysis using Dandelion revealed that the plasma cell clusters mostly contained a single pair of chains (93.81%), with orphan chains accounting for only a small fraction (2.65%), while immunoglobulin was primarily detected only in plasma and B cells (Fig. 1F and Supplementary Fig. 1A). The predominant immunoglobulin heavy chain (IGH) isotype expressed by B cells was IGHM ($n = 109$) (Fig. 1G), whereas that of plasma cells was IGHG1 ($n = 109$) (Fig. 1H and Supplementary Fig. 1B). The pairing frequency of heavy and light chains showed that the IGHM-IGKC combination was the most frequent combination in B cells, while the IGHG1-IGKC combination was the most frequent combination in plasma cells (Fig. 1G–H and Supplementary Fig. 2). Additionally, we identified a list of genes

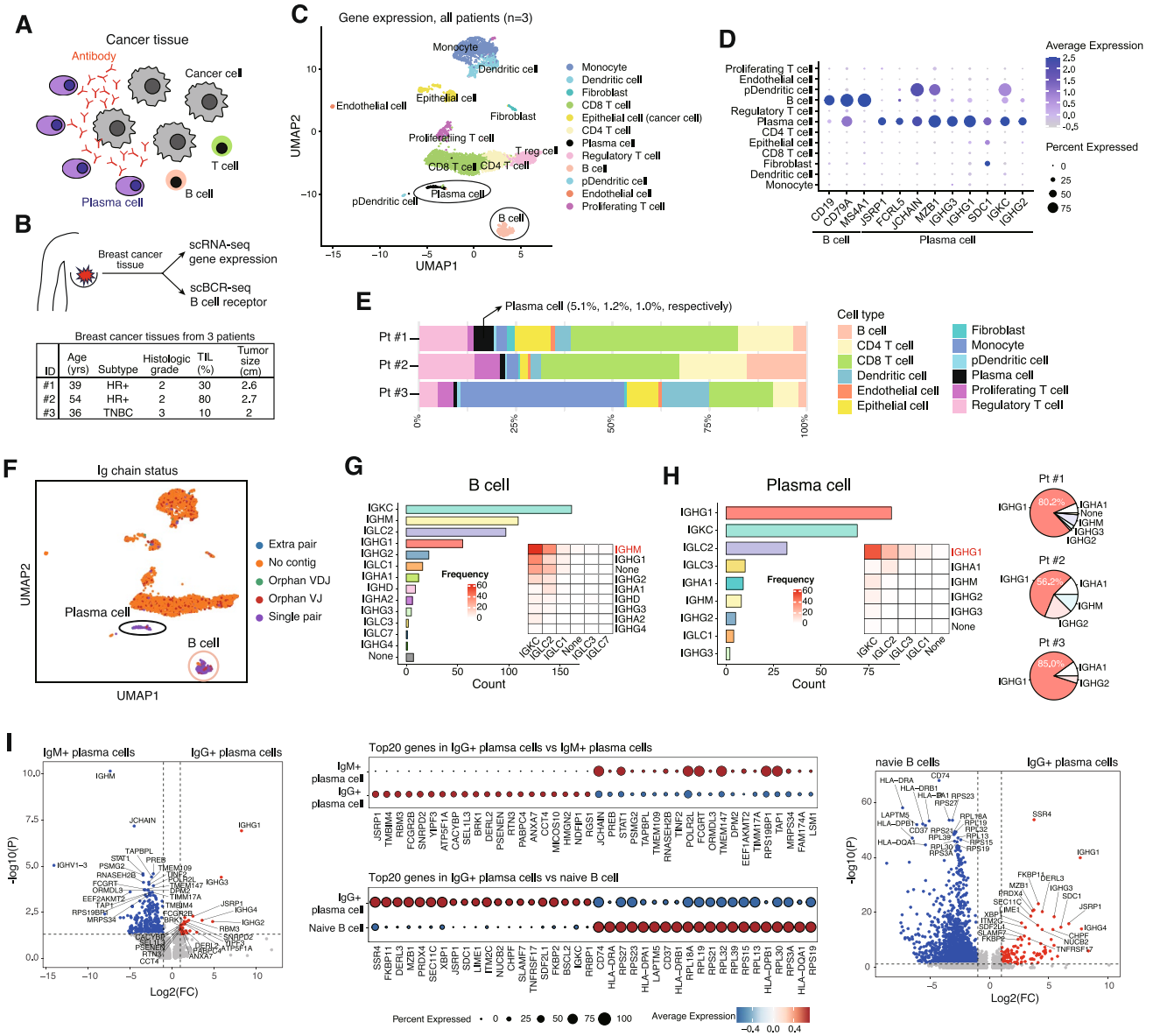

Fig. 1 Single-cell ribonucleic acid-seq gene expression (scRNA-seq) and single-cell B cell receptor (BCR) sequencing (scBCR-seq) in breast cancer tissue samples. **A** The schematics of the hypothesis: the infiltrated plasma cells in the tumor tissue would retain the RNA sequences for the cancer cell-associated antibody synthesis. **B** scRNA-seq and scBCR-seq were simultaneously performed on breast cancer tissue from three patients, two with hormone receptor (HR)-positive cancer and one with triple-negative breast cancer. **C** In clustering the scRNA-seq data, the plasma and B cell clusters are identified (circled). **D** The plasma cell cluster expresses known plasma cell markers, assuring the reliability of the clustering. **E** The proportions of each cell type from each patient. Plasma cells comprise 5.1%, 1.2%, and 1.0%, respectively. **F** In the pairing of immunoglobulin (Ig) heavy and light chains, a single pair was primarily identified in plasma and B cells; however, no Ig was detected in the other cells. **G** Frequencies of Ig isotypes and their pairing found in B cells. **H** Frequencies of Ig isotypes and their pairing found in plasma cells. The most commonly identified Ig isotypes are IGHG1 and IGKC for the heavy and light chains, respectively. **I** Gene lists differentially expressed in IgG$^+$ plasma cells compared with IgM$^+$ plasma or naïve B cells (Wilcoxon-rank sum test, two-tailed). The dot plots in the middle panel were generated, excluding the IGH-related genes

involved in the differentiation of IgM + plasma cells or naïve B cells into IgG + plasma cells (Fig. 1I). Differential gene expression analysis between the IgG + plasma cell and Naïve B cell confirmed that genes highly expressed in plasma cells, such as *XBP1* [21] and *SDC1* [22], were overexpressed in IgG + plasma cells.

Plasma cell infiltration as an effect of tumor immune response

We performed a cell-to-cell ligand-receptor interaction analysis using CellChat to investigate the association between plasma and cancer cells in the immune response within the tumor tissue and identified a strong interaction among pre-differentiation B, cluster of differentiation 4 (CD4) T, and cancer cells within the tumor tissues (Fig. 2A). In CellChat analysis, enhanced interactions between CD4 T cells and B cells via the MHC-II pathway was observed in tumor tissues (Fig. 2B and Supplementary Fig. 3A). Therefore, it is likely that the MHC-II pathway is activated through the interaction of various cells within the tumor tissue with notably high expression of human leukocyte antigen (HLA)-DRB1, which encodes the beta chain of MHC-II, and HLA-DRA, which encodes the alpha chain (Fig. 2C). The expression of CD40-CD40LG ligand and receptor genes, which promote the differentiation of B cells into plasma cells upon stimulation from CD4 T cells (Supplementary Fig. 3B), was well-identified in both B and CD4 T cells (Fig. 2D). Taken together, these findings suggest that the plasma cells within the cancer tissue samples were cancer-associated plasma cells induced by the immune response of the tumor-host.

Identification of plasma cell populations exhibiting clonal expansion and recombinant antibody synthesis

We performed a refined cluster analysis specifically on the plasma and B cell clusters, which allowed us to classify the cells into naïve B, B, and plasma cells (Fig. 3A and Supplementary Fig. 4). We then conducted a trajectory analysis, which revealed the differentiation from naïve B to B cells and finally to terminally differentiated plasma cells (Fig. 3B). We also observed that, as naïve B cells differentiated into plasma cells, the expression of IGHG1 increased while the expression of HLA-DRA gradually decreased (Fig. 3C). Next, we analyzed the clonality of plasma cells with Dandelion and observed that most of the cells forming clones were plasma cells (Fig. 3D). Based on this information, we selected six plasma cell clones with full Ig sequences to synthesize antibodies. Ab#1, produced from the plasma cell that formed the largest clone (Fig. 3E), originated from the most differentiated plasma cell (Fig. 3F) in the pseudotime trajectory analysis. The plasma cells that produced Ab#1 were mostly from patient 1; however, a few were also present in patient 3 (Fig. 3F), suggesting that shared antigens may exist across cancer

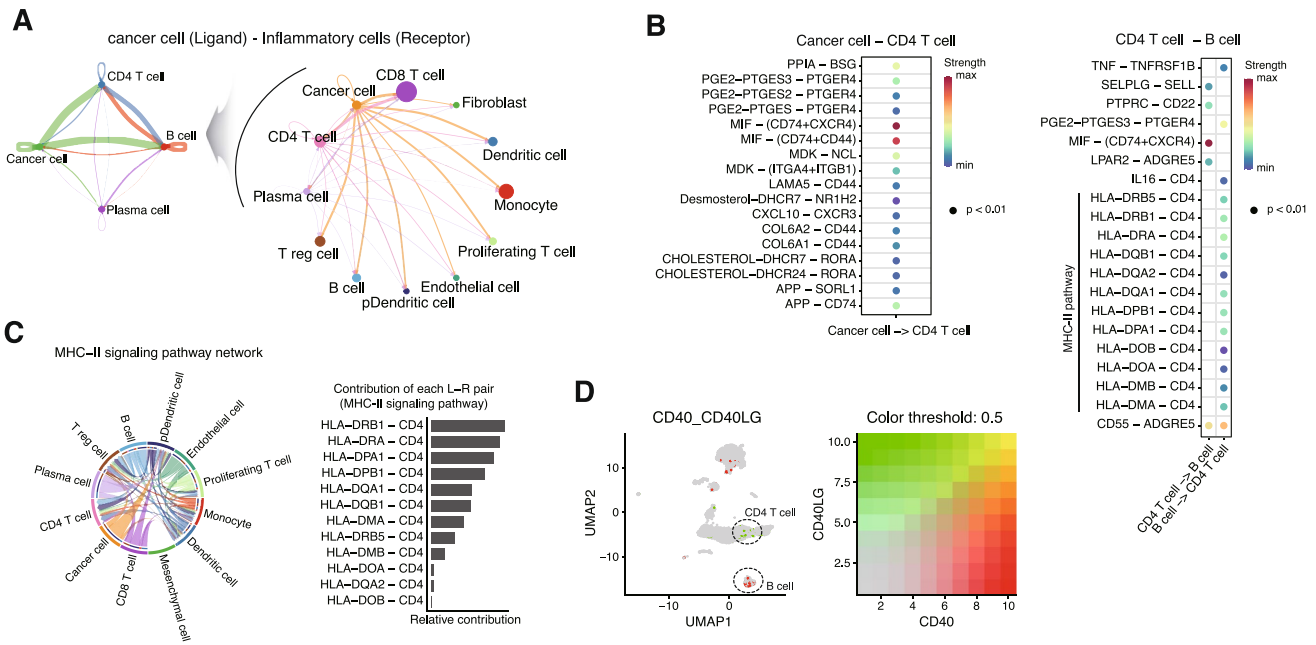

Fig. 2 Ligand-receptor interaction between cell types. **A** Strength of interaction among the cell types. A strong interaction of cancer cells with cluster of differentiation 4 (CD4) T and B cells indicates that the plasma cells infiltrating the tumor tissue are cancer-associated. **B** In cancer-associated CD4 T cells, a significant interaction with B cells through the major histocompatibility complex class II (MHC-II) pathway is present. **C** The MHC-II signaling pathway is activated through interaction between various immune and cancer cells in breast cancer tissues. Among the ligand (L)—receptor (R) pairs in the MHC-II pathway, the contribution of human leukocyte antigen (HLA)-DRB1 and HLA-DRA is the highest. **D** The expression of the CD40-CD40LG genes, which are crucial for the differentiation of B cells into plasma cells, shows that CD40 is primarily expressed in B cells, while CD40LG is primarily expressed in CD4 T cells, indicating an interaction between these two cell types

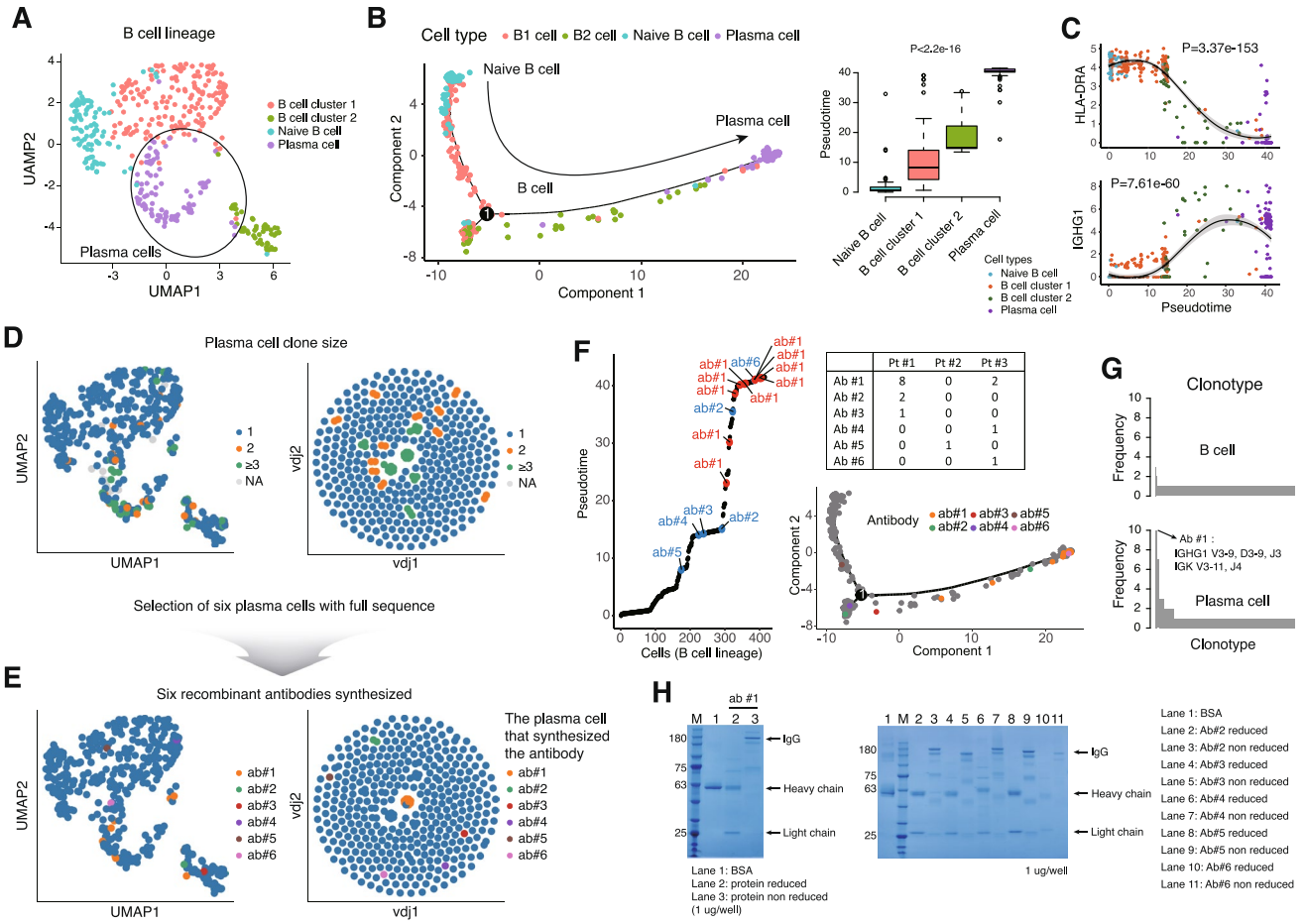

	Pt #1	Pt #2	Pt #3
Ab #1	8	0	2
Ab #2	2	0	0
Ab #3	1	0	0
Ab #4	0	0	1
Ab #5	0	1	0
Ab #6	0	0	1

Fig. 3 Antibody synthesis using antibody sequences from plasma cells with clonal expansion. **A** Uniform manifold approximation and projection (UMAP) clustering on the B cells further identifies three lineages of the B cells—naïve B, B, and plasma cells. **B** Pseudotime trajectory analysis confirmed that plasma cells are the most differentiated among the B cell lineage (Spearman correlation test, two-tailed). **C** The expression of IGHG1 increases during the differentiation of B cells to plasma cells, whereas the expression of HLA-DRA decreases (Spearman correlation test, two-tailed). **D** B cell receptor clonality and their sizes. Cells that form two or more clones are predominantly plasma cells. **E** Six plasma cell clones selected for antibody synthesis, including antibody 1 (Ab#1), which formed the largest clone size. **F** Pseudotime trajectory analysis shows that Ab#1 is the most differentiated and predominantly identified clone from patients 1 and 3. **G** Clonotype frequency in B and plasma cells. The frequency of clonotypes is higher in plasma cells, and Ab#1 was synthesized from the clonotype with the highest frequency. **H** Production of recombinant antibodies for a total of six antibodies

tissues among patients. In the clonotype analysis, cells with the same clonotype were more frequently found in plasma cells than in B cells, with the plasma cells expressing Ab#1 forming the largest group of the same clonotype, suggestive of clonal expansion (Fig. 3G). The presence of antibodies, such as Ab#1, generated by plasma cells showing clonal expansion among multiple clones suggests its potential involvement in a strong immune response, possibly contributing to tumor-specific interactions. We then synthesized the recombinant antibodies through cloning based on the sequences of the six antibodies from the selected plasma cell clones (Fig. 3H and Supplementary Table 2). In the protein electrophoresis experiment, samples with a reducing agent were labeled as "reduced," while those without were labeled as "non-reduced." The reducing agent was used to break disulfide bonds, allowing the visualization of separate light and heavy chain bands in the gel (Fig. 3H).

Results of immunohistochemical staining of cancer tissues with the corresponding synthesized antibodies

We performed immunohistochemistry with the synthesized antibodies on the cancer tissues previously analyzed by scBCR-seq (Fig. 3F). Tonsil tissue was used as a negative control for the antibodies (Supplementary Fig. 5A). After immunostaining the tumor tissues with the synthesized Ab#1, staining was observed along the cell membrane in the cancer cells from patients 1 and 3, where plasma cells were

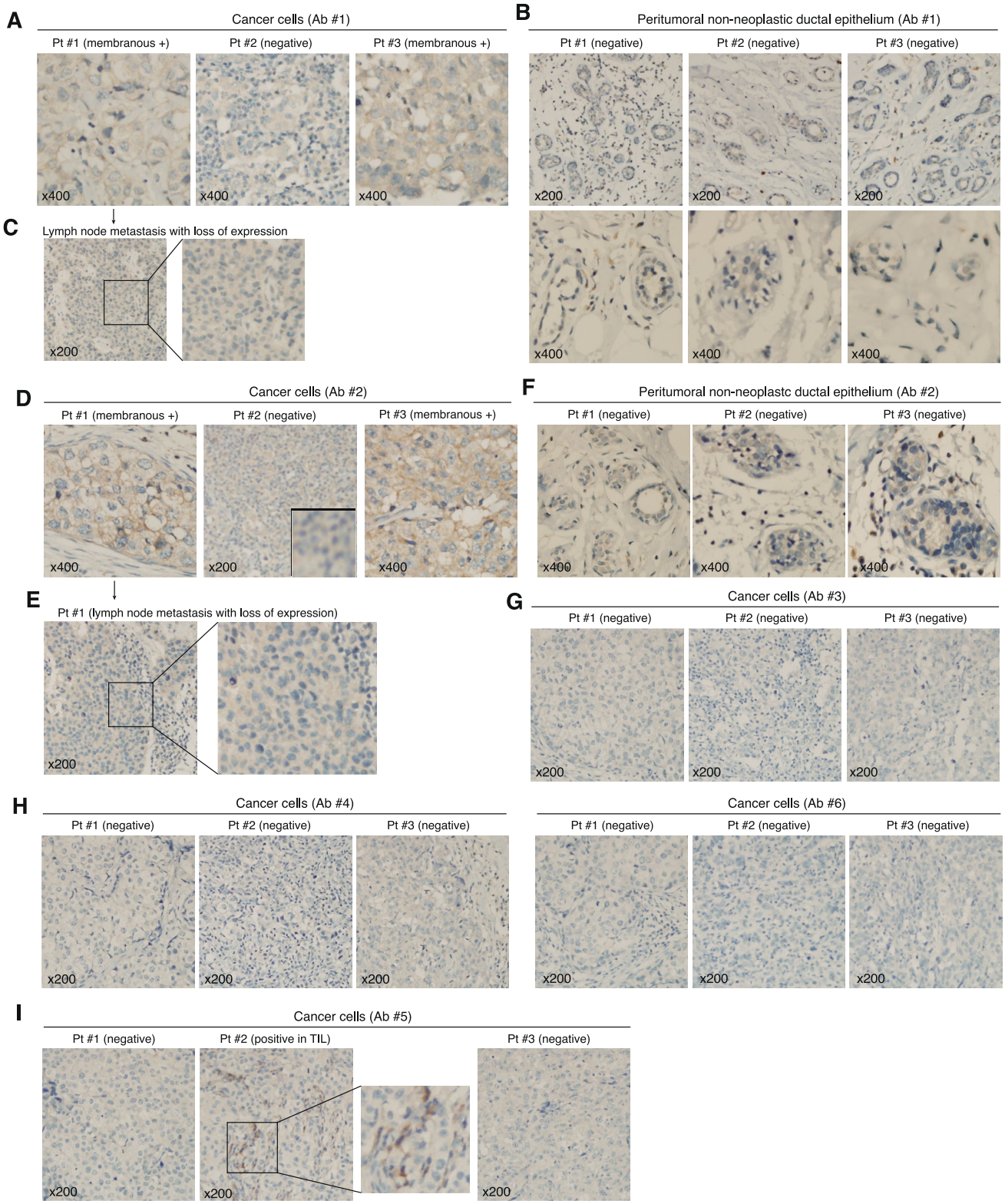

present; however, no membranous staining was observed in the cancer cells from patient 2 (Fig. 4A). Additionally, no immunostaining was observed in the normal ductal epithelial cells around the tumors in any of the three patients (Fig. 4B). However, a loss of expression was shown in the cancer cells that metastasized to the lymph node of patient 1 (Fig. 4C). Ab#2 also showed membranous staining in the cancer cells of patients 1 and 3, although the associated plasma cells

◂**Fig. 4** Immunohistochemical staining results of the synthesized antibodies. **A** Immunostaining results of Ab#1 in cancer tissues. Membranous staining was observed in cancer cells from patients 1 and 3. **B** Peritumoral normal ductal epithelium showed negative staining. **C** A loss of expression was observed in the cancer cells that had metastasized to the lymph nodes. **D** Immunostaining results for Ab#2. Membranous staining was observed in the cancer cells from patients 1 and 3. **E** A loss of expression for Ab#2 was observed in the cancer cells that had metastasized to the lymph nodes. **F** Peritumoral normal ductal epithelium showed negative staining. **G**, **H**, **I** Immunostaining results for the remaining four antibodies. All ductal epithelium showed negative staining, and some lymphocytic cells displayed positive cytosolic staining

were not identified in patient 3 (Fig. 4D). Again, no staining was observed in patient 2. Similar to Ab#1, a decreased expression was observed in the cancer cells with lymph node metastasis (Fig. 4E). The Ab#2 did not stain the peritumoral normal ductal epithelium (Fig. 4F). Additionally, we identified that neither Ab#1 nor Ab#2 stained the normal ductal epithelium in 103 independent normal breast tissue samples (Supplementary Fig. 5B). We selected four additional plasma cells that did not form clones, where full sequences for both heavy and light chains were identified and the sequences or isotypes differed. Then, four different antibodies were synthesized using the antibody sequence information from these plasma cells. These antibodies, Ab#3, #4, #5, and #6, were derived from plasma cells that did not undergo clonal expansion, and none of them showed immunostaining within the cancer tissues (Fig. 4 G H, I). The antibodies exhibited a cytosolic expression pattern in lymphocytic cells within the tumor tissues (Fig. 4I).

Clinical significance of plasma cell infiltration in breast cancer

To evaluate the clinical significance of plasma cell infiltration, we identified a plasma cell signature gene set from scRNA-seq data (Fig. 5A and Supplementary Table 3). Using this gene set, we performed deconvolution on TCGA bulk RNA-seq data of breast cancer to calculate plasma cell scores (Fig. 5A). Additionally, a pathologist classified the degree of plasma cell infiltration (little, mild, moderate, or marked) in the histological images form the TCGA breast cancer dataset (Fig. 5B). We confirmed that the plasma cell scores derived from the RNA-seq expression data significantly correlated with the actual degree of plasma cell infiltration observed histologically (Fig. 5C). Additionally, this plasma cell score showed a significant correlation with the plasma cell score obtained using CIBERSORT (Fig. 5D). Plasma cell infiltration was associated with the immunogenic mutation burden of the cancer cells, which can generate novel peptide sequences and potentially impact the immune response and plasma cell infiltration (Fig. 5E). Patients with high plasma cell infiltration in their breast cancer tissue specimens exhibited a favorable prognosis (Fig. 5F), even after adjusting for other clinical variables including age, sex, tumor staging, and tumor histologic type (Fig. 5G). Plasma cell infiltration may, therefore, be an independent prognostic factor, suggesting the high clinical applicability of antibody synthesis.

Clinical significance of IGH isotype in breast cancer

The prognostic significance of plasma cell infiltration within tumor tissue has been identified not only in breast cancer but also among other cancers (Fig. 6A), indicating the substantial clinical importance of plasma cells. In this study, plasma cells most commonly secreted the IGHG1 isotype; therefore, we further investigated the clinical significance of this specific isotype. Using an in-house analysis pipeline, we measured the relative abundance of IGH isotypes from raw RNA-seq FASTQ files (Fig. 6B). Among the various IGH isotypes analyzed, IGHG1 showed the strongest correlation with plasma cell score, suggesting that plasma cells within the cancer tissue primarily secrete IGHG1 (Fig. 6C). Although IGHG1 was the most abundantly secreted isotype in breast cancer tissues, the amount secreted varied among patients (Fig. 6D). Furthermore, patients with high levels of secreted IGHG1 in breast cancer tissues exhibited favorable prognoses (Fig. 6E); therefore, the level of IGHG1 secretion also served as an independent prognostic factor (Fig. 6F). Similar to scRNA-seq data, HLA-DRA had the highest expression among the MHC-II class molecules observed in the breast cancer tissue samples, which was significantly correlated with IGHG1 isotype expression (Fig. 6G). Additionally, increased BCR diversity within tumor tissues correlated with higher IGHG1 expression (Fig. 6H), which may suggest that tumors with higher IGHG1 expression have a more robust or active immune response, potentially influencing the behavior of the tumor and the prognosis of the patient. Breast cancers with high IGHG1 expression are characterized by increased immunogenic mutation burden, intratumoral heterogeneity, and aneuploidy scores (Fig. 6I), all of which are characteristics associated with high tumor immunogenicity. When examining the association between the somatic mutations of breast cancer [23] and intratumoral IGHG1 expression, the *TP53* mutation among known driver mutations showed the strongest association with high IGHG1 expression (Fig. 6J). Therefore, the increased IGHG1 levels associated with these traits suggest that IGHG1 may be linked to the products of immune responses associated with cancer cells.

Discussion

In this study, we analyzed the role of plasma cell infiltration in breast cancer using scRNA-seq and scBCR-seq. Our findings provide some insights into the immune landscape

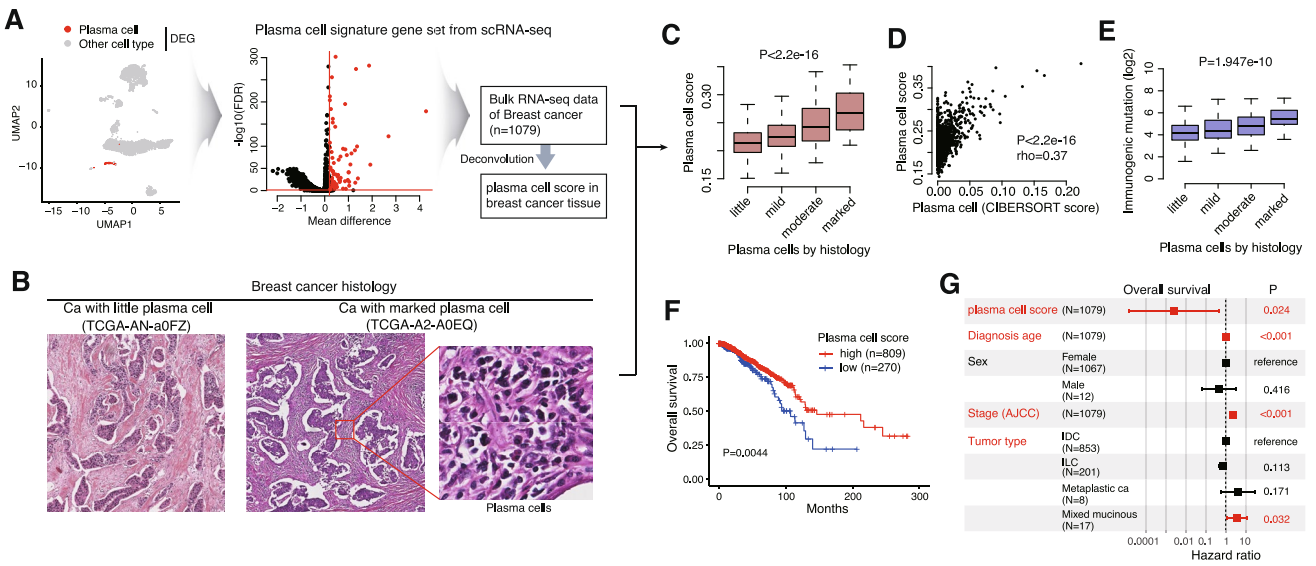

Fig. 5 Clinical significance of plasma cell infiltration in breast cancer tissue. **A** Plasma cell scores of the bulk RNA-seq data from 1,079 patients with breast cancer using the plasma cell signature genes identified from single-cell RNA-seq. **B** Histological analysis of the patient tissue slides to classify their plasma cell infiltration levels (little, mild, moderate, and marked). Tissues were stained in hematoxylin and eosin. The most representative images from two patients (TCGA-AN-a0FZ and TCGA-A2-A0EQ) are shown. **C** Plasma cell scores and infiltration levels by histology reveal a significant positive correlation (Spearman correlation test, two-tailed). **D** A significant correlation between the plasma cell score developed in this study and the CIBERSORT plasma cell score (Spearman correlation test, two-tailed). **E** The plasma cell infiltration levels also show a significant positive correlation with immunogenic tumor mutation burdens (Spearman correlation test, two-tailed). **F** Patients with high levels of plasma cell infiltration have a significantly better prognosis than patients with lower levels of plasma cell infiltration (log-rank test, two-tailed). **G** Multiple Cox regression analysis with numerous clinical variables suggest that plasma cell infiltration could be an independent prognostic factor

of breast cancer and suggest the potential of plasma cells as key components of the tumor microenvironment. Integrating scRNA-seq and scBCR-seq allowed us to identify the specific gene signatures and BCR repertoires associated with plasma cells. Plasma cells expressed high levels of IGHG1 and IGKC, indicating the predominance of the specific Ig isotypes response within the tumor microenvironment.

Cell type annotation such as plasma cells and naive B cells from scRNA-seq data was validated by differential gene expression analysis, which showed that genes such as *XBP1* [21] and *SDC1* [22] were overexpressed in plasma cells, indicating appropriate cell type classification. Additionally, the mechanism of isotype switching from IgM to IgG is not yet well understood. Through differential gene expression analysis, we aimed to highlight how gene expression differs between these two isotypes. Although well-known genes involved in isotype switching, such as *IRF4* and *PRDM1* [24], were not included in our top 20 differentially expressed genes, several of the top genes were associated with cell differentiation (*YIPF3*), and cell survival (*CCT4, TMBIM4*). The increased survival signals in IgG + plasma cells suggest that this isotype of plasma cells is involved in long-term immunity.

Using scRNA-seq data, we investigated the ligand-receptor interactions between cancer-associated plasma cells and other cell types within the tumor tissues and found that cancer cells strongly interacted with CD4 T and B cells. Although we could not directly observe the immune response process leading to anti-tumor antibody production, our scRNA-seq data analysis suggests the presence of interactions between B cells and CD4 T cells. This implies that B cell differentiation may occur within the tumor microenvironment. In the pseudotime trajectory analysis, we observed that the antibody clones, particularly Ab#1, exhibited marked clonal expansion and differentiation, predominantly in patient 1. This clonal proliferation suggests that specific antibody clones may play a role in mediating immune responses against tumor cells. Immunostaining with Ab#1 and #2, identified as having a clonal expansion, showed membranous staining in cancer cells but not in normal cells, suggesting that these antibodies may be cancer-associated antibodies. Although further validation is required to determine the clinical applicability of these antibodies, the results of this study imply that this approach could potentially be useful in the identification of cancer-associated antibodies. A study by Katoh et al. [25] on the utility of identifying cancer-associated antibodies in cancer tissues supports our findings. Furthermore, several studies [7, 26–28] which have demonstrated that the intratumoral immune response propagates tumor-oriented immunoglobulin clones and presents

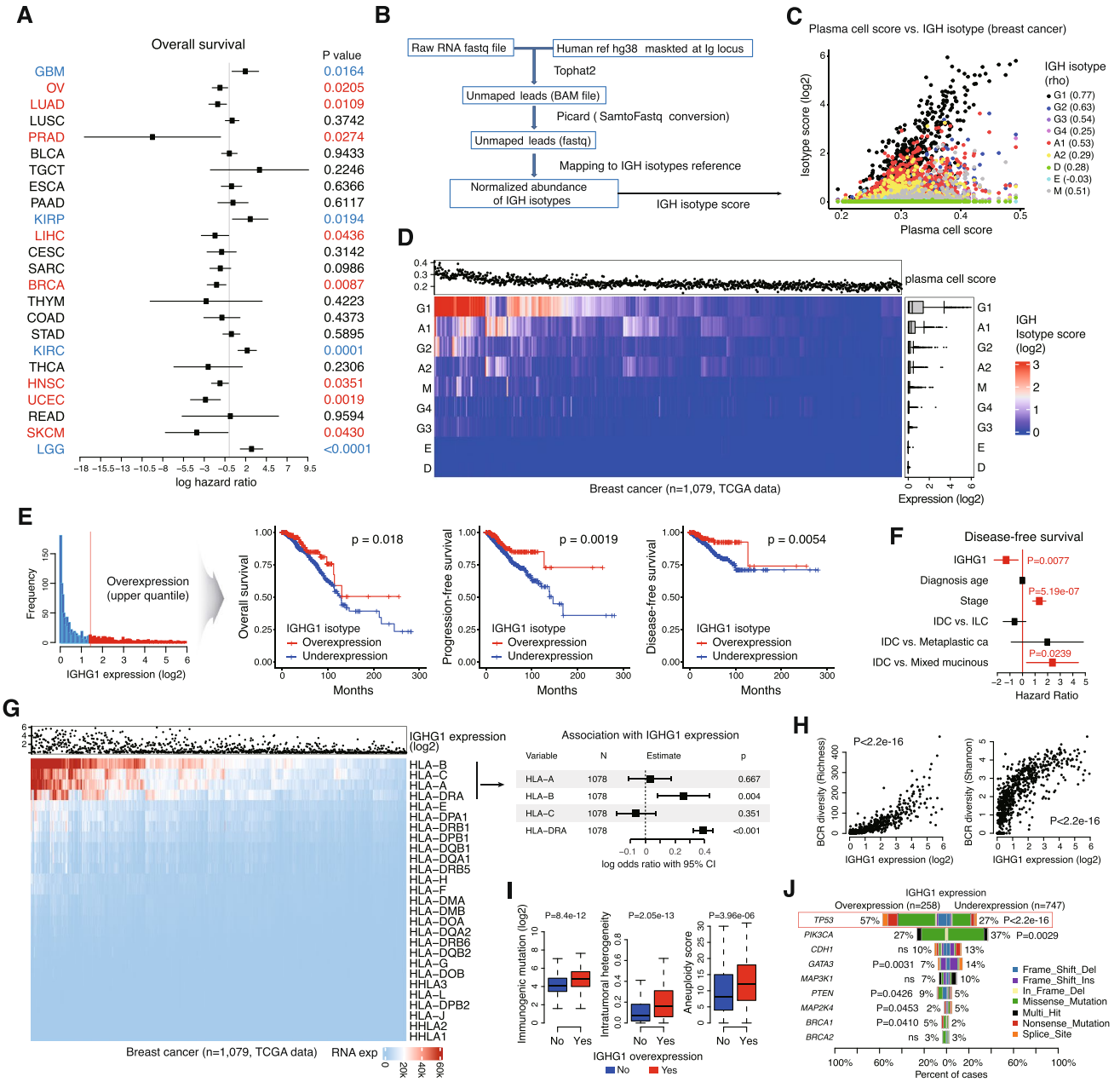

Fig. 6 Clinical significance of IGHG1 isotype. **A** The infiltration of plasma cells within tumors was associated with favorable prognosis in various cancers, including breast cancer (univariate Cox regression analysis). **B** An analysis pipeline for measuring the abundance of IGH isotypes (IGH isotype score) within tumors from bulk RNA sequencing data. **C** Among the various isotypes, IGHG1 showed the highest correlation with the plasma cell score (Spearman correlation test, two-tailed). **D** Among the various IGH isotypes, IGHG1 is the most abundant among 1,079 breast cancer tissues. **E** When the IGHG1 score was divided based on the upper quantile, tumors with higher IGHG1 scores had better overall, progression-free, and disease-free survival (Log-rank test, two-tailed). **F** IGHG1 remained independently significant for survival even after adjusting for other clinical variables such as stage (multiple Cox regression analysis). **G** Among the MHC-II class genes, HLA-DRA had the highest expression and significantly correlated with the IGHG1 score (Multiple linear regression analysis). **H** IGHG1 score was significantly correlated with BCR diversity (Spearman correlation test, two-tailed). **I** Tumors with higher IGHG1 scores are associated with increased immunogenic mutations, intratumoral heterogeneity, and levels of aneuploidy (Wilcoxon-rank sum test, two-tailed). **J** Association between mutations and IGHG1 levels in breast cancers (Fisher exact test, two-tailed)

a therapeutic approach for human malignancies also underscore the potential significance of cancer-associated antibodies identified in our study.

An unexpected observation was that the same antibody clone was isolated from two of the three patients. This can be partially explained by the study conducted by Furuya

et al. [25], which described that anti-densely sulfated glycosaminoglycans/nucleic acids clones found in cancer tissues frequently and specifically react with various human malignancies, suggesting the possibility of cancer-associated clones shared among patients. In a study on pancreatic cancer, Yao et al. [28] identified that the antigens found within the tumor were self-antigens, such as F-actin and Hsp60, leading to the production of autoantibodies that reacted with the antigens. Therefore, the cross-reactivity observed in our study may be due to an immune response against self-antigens. However, since immunostaining was not observed in the control healthy tissues, the antibodies are likely associated with tumor cells. One limitation of our study, however, is the lack of identification of the specific antigen bound to the antibodies.

In this study, primary cancer cells showed immunostaining for the antibodies, whereas cancer cells in the lymph nodes exhibited reduced immunostaining. This could be related to the evasion of the host immune system by the cancer cells. However, further research is needed to explore this connection.

Cancer encompasses a complex cellular microenvironment in which the interactions among the numerous cell types are pivotal in shaping disease progression and therapeutic responses [13, 26, 27, 29]. Although breast cancer typically exhibits a low mutational burden and limited immunogenicity, immune activation remains crucial for a subset of patients [30]. TILs, for instance, have been recognized as biomarkers associated with positive clinical outcomes and a complete pathological response to neoadjuvant chemotherapy [31]. The results of our study demonstrated a significant correlation between plasma cell infiltration and tumor mutation burden, suggesting that increased plasma cell infiltration is associated with increased tumor mutation burden. This relationship indicates that plasma cells may respond to a higher mutational load by producing a diverse array of antibodies, potentially enhancing anti-tumor immunity. Moreover, patients with high plasma cell scores exhibited improved overall survival, underscoring the prognostic value of plasma cell infiltration in breast cancer. Multivariable analysis confirmed that plasma cell scores were significant predictors of patient outcomes, highlighting plasma cell infiltration as a potential independent prognostic factor.

In our study, IGHG1 was observed as the most abundant isotype, and high intratumoral IGHG1 expression has been reported to be associated with favorable prognosis in breast cancer, melanoma, and lung cancer [32–34]. Additionally, IgG1 has the highest FcγR-binding affinity among the IgG isotypes, which enables it to effectively induce antibody-dependent cell-mediated cytotoxicity (ADCC) [35]. These suggest that IGHG1 is related to an active immune response in tumor. In particular, in lung adenocarcinoma with *KRAS* mutations, high IGHG1 expression was associated with prolonged survival and this may result from the efficient presentation of mutant *KRAS* peptides by abundant IgG1 tumor-infiltrating B cells [33]. The recent identification of *KRAS* mutation-specific CD4 + T cells and the ability of tumor-infiltrating B cells to present antigens and activate CD4 + T cells suggest that IgG B cells may play a role in antitumor immunity [36, 37]. In the breast cancer mutation data analysis, tumors with high IGHG1 isotype expression exhibited a significantly higher frequency of *TP53* mutations. Associations with other driver gene mutations may also suggest that IgG1 B cells are linked to tumor characteristics. Furthermore, the decreased immunostaining observed in lymph node metastatic tumors in our study may be related to differences in the mutation profiles between metastatic and primary tumors [38].

Our study has several limitations. First, the number of donors analyzed in the single-cell sequencing for antibody identification was limited to three, which may restrict the ability to draw significant conclusions. Second, the lack of functional validation experiments for the identified antibodies or their binding antigens is another limitation. Additionally, we did not assess the specificity of the antibodies in various normal tissues beyond breast tissue, which limits the comprehensive validation of their cancer specificity.

Conclusions

Our study provides an analysis of plasma cell infiltration in breast cancer, revealing its significant association with prognosis. The integration of scRNA-seq and scBCR-seq has uncovered insight into the immune dynamics within the tumor microenvironment, highlighting the potential of IGHG1-expressing plasma cells as potential biomarkers and immunotherapy targets by identifying cancer-associated antibodies.

Supplementary Information The online version contains supplementary material available at https://doi.org/10.1007/s00262-025-04045-9.

Acknowledgements We thank the Antibody Development core facility and the Bioinformatics core facility at the ConveRgence mEDIcine research cenTer (CREDIT), Asan Medical Center for support and instrumentation.

Author contributions COS: conceptualization. COS, JHK, HJL: supervision and organization. COS and HJL: funding and material provisions. WK and COS: data analysis, interpretation, prepared all figures, and writing of original draft. JHO, CWP, YGK, DEO, and JHK: assistance with analysis, data interpretation, and writing. HK: recombinant antibody production. All authors reviewed the manuscript.

Funding This study was supported by grants from the Basic Science Research Program of the National Research Foundation of Korea (no. NRF-RS-2024-00338555, RS-2024-00334460, RS-2023-00275813, and RS-2025-00557349); grants from the Asan Institute for Life Sciences of Asan Medical Center (nos. 2023IP0083-2 and 2024IP0082-1);

and a grant of the Korea Health Technology R&D Project through the Korea Health Industry Development Institute (KHIDI), funded by the Ministry of Health & Welfare, Republic of Korea (no. HR21C0198).

Data availability Single-cell RNA sequencing data and CDR sequences for tested antibodies may available upon reasonable request. The datasets generated and/or analyzed during the present study are available from the corresponding authors upon reasonable request. Other bulk RNA sequencing data used in this study are available in the public domain at https://portal.gdc.cancer.gov/.

Declarations

Conflict of interests The authors declare that they have no conflict of interests.

Ethical approval This study was approved by the institutional review board (IRB) of Asan Medical Center (IRB no.2015–0438).

Consent to participate Written informed consent was obtained from all participants, and all methods were carried out in accordance with the relevant guidelines and regulations.

Consent to publication A statement confirming that consent to publish has been received from all participants should appear in the manuscript.

References

1. Hendriks D, Choi G, de Bruyn M, Wiersma VR, Bremer E (2017) Antibody-based cancer therapy: successful agents and novel approaches. Int Rev Cell Mol Biol 331:289–383. https://doi.org/10.1016/bs.ircmb.2016.10.002
2. Alt FW, Zhang Y, Meng FL, Guo C, Schwer B (2013) Mechanisms of programmed DNA lesions and genomic instability in the immune system. Cell 152:417–429. https://doi.org/10.1016/j.cell.2013.01.007
3. Azizi E, Carr AJ, Plitas G et al (2018) Single-cell map of diverse immune phenotypes in the breast tumor microenvironment. Cell 174:1293–308.e36. https://doi.org/10.1016/j.cell.2018.05.060
4. Sade-Feldman M, Yizhak K, Bjorgaard SL et al (2018) Defining T cell states associated with response to checkpoint immunotherapy in melanoma. Cell 175:998-1013.e20. https://doi.org/10.1016/j.cell.2018.10.038
5. Li H, van der Leun AM, Yofe I et al (2019) Dysfunctional CD8 T cells form a proliferative, dynamically regulated compartment within human melanoma. Cell 176:775–89.e18. https://doi.org/10.1016/j.cell.2018.11.043
6. Guo X, Zhang Y, Zheng L et al (2018) Global characterization of T cells in non-small-cell lung cancer by single-cell sequencing. Nat Med 24:978–985. https://doi.org/10.1038/s41591-018-0045-3
7. Patil NS, Nabet BY, Müller S et al (2022) Intratumoral plasma cells predict outcomes to PD-L1 blockade in non-small cell lung cancer. Cancer Cell 40:289-300.e4. https://doi.org/10.1016/j.ccell.2022.02.002
8. Wouters MCA, Nelson BH (2018) Prognostic significance of tumor-infiltrating B cells and plasma cells in human cancer. Clin Cancer Res 24:6125–6135. https://doi.org/10.1158/1078-0432.Ccr-18-1481
9. Sakaguchi A, Horimoto Y, Onagi H et al (2021) Plasma cell infiltration and treatment effect in breast cancer patients treated with neoadjuvant chemotherapy. Breast Cancer Res 23:99. https://doi.org/10.1186/s13058-021-01477-w
10. Kuroda H, Jamiyan T, Yamaguchi R, Kakumoto A, Abe A, Harada O, Enkhbat B, Masunaga A (2021) Prognostic value of tumor-infiltrating B lymphocytes and plasma cells in triple-negative breast cancer. Breast Cancer 28:904–914. https://doi.org/10.1007/s12282-021-01227-y
11. Kroeger DR, Milne K, Nelson BH (2016) Tumor-infiltrating plasma cells are associated with tertiary lymphoid structures, cytolytic t-cell responses, and superior prognosis in ovarian cancer. Clin Cancer Res 22:3005–3015. https://doi.org/10.1158/1078-0432.Ccr-15-2762
12. Hendry S, Salgado R, Gevaert T et al (2017) Assessing tumor-infiltrating lymphocytes in solid tumors: a practical review for pathologists and proposal for a standardized method from the international immunooncology biomarkers working group: part 1: assessing the host immune response, TILs in invasive breast carcinoma and ductal carcinoma in situ, metastatic tumor deposits and areas for further research. Adv Anat Pathol 24:235–251. https://doi.org/10.1097/pap.0000000000000162
13. Cho SJ, Oh JH, Baek J et al (2023) Intercellular cross-talk through lineage-specific gap junction of cancer-associated fibroblasts related to stromal fibrosis and prognosis. Sci Rep 13:14230. https://doi.org/10.1038/s41598-023-40957-1
14. Choi JI, Cho EJ, Yang MJ, Noh HJ, Park SH, Kim S, Kim YS, Sung CO, Lee D (2023) Hypoxic microenvironment determines the phenotypic plasticity and spatial distribution of cancer-associated fibroblasts. Clin Transl Med 13:e1438. https://doi.org/10.1002/ctm2.1438
15. Jin S, Guerrero-Juarez CF, Zhang L, Chang I, Ramos R, Kuan CH, Myung P, Plikus MV, Nie Q (2021) Inference and analysis of cell-cell communication using cell chat. Nat Commun 12:1088. https://doi.org/10.1038/s41467-021-21246-9
16. Thorsson V, Gibbs DL, Brown SD et al (2018) The immune landscape of cancer. Immunity 48:812–30.e14. https://doi.org/10.1016/j.immuni.2018.03.023
17. Wilks C, Cline MS, Weiler E et al (2014) The cancer genomics hub (CGHub): overcoming cancer through the power of torrential data. Database. https://doi.org/10.1093/database/bau093
18. Kim D, Pertea G, Trapnell C, Pimentel H, Kelley R, Salzberg SL (2013) TopHat2: accurate alignment of transcriptomes in the presence of insertions, deletions and gene fusions. Genome Biol 14:R36. https://doi.org/10.1186/gb-2013-14-4-r36
19. Langmead B, Salzberg SL (2012) Fast gapped-read alignment with Bowtie 2. Nat Methods 9:357–359. https://doi.org/10.1038/nmeth.1923
20. Li H, Handsaker B, Wysoker A, Fennell T, Ruan J, Homer N, Marth G, Abecasis G, Durbin R (2009) The sequence alignment/map format and SAMtools. Bioinformatics 25:2078–2079. https://doi.org/10.1093/bioinformatics/btp352
21. Iwakoshi NN, Lee AH, Vallabhajosyula P, Otipoby KL, Rajewsky K, Glimcher LH (2003) Plasma cell differentiation and the

unfolded protein response intersect at the transcription factor XBP-1. Nat Immunol 4:321–329. https://doi.org/10.1038/ni907
22. Shaffer AL, Shapiro-Shelef M, Iwakoshi NN et al (2004) XBP1, downstream of Blimp-1, expands the secretory apparatus and other organelles, and increases protein synthesis in plasma cell differentiation. Immunity 21:81–93. https://doi.org/10.1016/j.immuni.2004.06.010
23. Ellrott K, Bailey MH, Saksena G et al (2018) Scalable open science approach for mutation calling of tumor exomes using multiple genomic pipelines. Cell Syst 6:271–81.e7. https://doi.org/10.1016/j.cels.2018.03.002
24. Ambegaonkar AA, Holla P, Sohn H, George R, Tran TM, Pierce SK (2024) Isotype switching in human memory B cells sets intrinsic antigen-affinity thresholds that dictate antigen-driven fates. Proc Natl Acad Sci U S A 121:e2313672121. https://doi.org/10.1073/pnas.2313672121
25. Furuya G, Katoh H, Atsumi S et al (2023) Nucleic acid-triggered tumoral immunity propagates pH-selective therapeutic antibodies through tumor-driven epitope spreading. Cancer Sci 114:321–338. https://doi.org/10.1111/cas.15596
26. Choi WS, Kwon HJ, Yi E et al (2024) HPK1 dysregulation-associated NK cell dysfunction and defective expansion promotes metastatic melanoma progression. Adv Sci (Weinh) 11:e2400920. https://doi.org/10.1002/advs.202400920
27. Sorlie T, Tibshirani R, Parker J et al (2003) Repeated observation of breast tumor subtypes in independent gene expression data sets. Proc Natl Acad Sci USA 100:8418–8423. https://doi.org/10.1073/pnas.0932692100
28. Yao M, Preall J, Yeh JT et al (2023) Plasma cells in human pancreatic ductal adenocarcinoma secrete antibodies against self-antigens. JCI Insight. https://doi.org/10.1172/jci.insight.172449
29. Park HJ, Cho EJ, Kim JH, Lim S, Sung CO (2023) Reshaping tumor immune microenvironment by Epstein-Barr virus activation in the stroma of colorectal cancer. iScience 26:105919. https://doi.org/10.1016/j.isci.2022.105919
30. Onkar SS, Carleton NM, Lucas PC, Bruno TC, Lee AV, Vignali DAA, Oesterreich S (2023) The great immune escape: understanding the divergent immune response in breast cancer subtypes. Cancer Discov 13:23–40. https://doi.org/10.1158/2159-8290.Cd-22-0475
31. Dushyanthen S, Beavis PA, Savas P, Teo ZL, Zhou C, Mansour M, Darcy PK, Loi S (2015) Relevance of tumor-infiltrating lymphocytes in breast cancer. BMC Med 13:202. https://doi.org/10.1186/s12916-015-0431-3
32. Larsson C, Ehinger A, Winslow S et al (2020) Prognostic implications of the expression levels of different immunoglobulin heavy chain-encoding RNAs in early breast cancer. NPJ Breast Cancer 6:28. https://doi.org/10.1038/s41523-020-0170-2
33. Isaeva OI, Sharonov GV, Serebrovskaya EO, Turchaninova MA, Zaretsky AR, Shugay M, Chudakov DM (2019) Intratumoral immunoglobulin isotypes predict survival in lung adenocarcinoma subtypes. J Immunother Cancer 7:279. https://doi.org/10.1186/s40425-019-0747-1
34. Bolotin DA, Poslavsky S, Davydov AN et al (2017) Antigen receptor repertoire profiling from RNA-seq data. Nat Biotechnol 35:908–911. https://doi.org/10.1038/nbt.3979
35. Yu J, Song Y, Tian W (2020) How to select IgG subclasses in developing anti-tumor therapeutic antibodies. J Hematol Oncol 13:45. https://doi.org/10.1186/s13045-020-00876-4
36. Cafri G, Yossef R, Pasetto A et al (2019) Memory T cells targeting oncogenic mutations detected in peripheral blood of epithelial cancer patients. Nat Commun 10:449. https://doi.org/10.1038/s41467-019-08304-z
37. Bruno TC, Ebner PJ, Moore BL et al (2017) Antigen-presenting intratumoral B cells affect CD4(+) TIL phenotypes in non-small cell lung cancer patients. Cancer Immunol Res 5:898–907. https://doi.org/10.1158/2326-6066.Cir-17-0075
38. Angus L, Smid M, Wilting SM et al (2019) The genomic landscape of metastatic breast cancer highlights changes in mutation and signature frequencies. Nat Genet 51:1450–1458. https://doi.org/10.1038/s41588-019-0507-7